FINITE ELEMENT MODELLING OF

NON-PENETRATING THORACIC IMPACT

I.S. Bush and S.A. Challener
Frazer-Nash Consultancy Limited
Randalls Way
Leatherhead
Surrey KT22 7TX
England

ABSTRACT

A study has been undertaken to identify the fundamental mechanisms involved during non-penetrating thoracic impact and in particular to determine how energy is transfered from the contact point on the thoracic wall to other sites inside the thorax.

Modelling of the thorax has been performed using the dynamic finite element codes DYNA2D and DYNA3D and the system modelling package GENDYN. Particular consideration has been given to the mechanisms by which pressure waves are generated, the propagation of these waves through the lung, parenchyma and the likely biophysical mechanisms involved in vascular injury.

The finite element method has been used to demonstrate the propagation of the pressure wave through the lung, including reflection at boundaries, and identifying regions where stress concentration and contusion damage may occur.

1. INTRODUCTION

It is well known that thoracic impacts can cause significant pulmonary contusion injuries even when no permanent damage is apparent at the impact site. Further, it has been found that the severity of injury is dependent on rather more than just the degree of deformation of the chest, factors such as impact velocity being at least as important[1]. However, although the results of thoracic impact are well documented, there is much less understanding of the reasons for observed behaviour.

A study has been carried out by Frazer-Nash Consultancy Limited (sponsored by the Chemical Defence Establishment, MOD (PE), Porton Down, England) to identify the mechanisms which contribute to lung injury under non-penetrating thoracic impact. The success of this study has enabled the behaviour to be explained more fully and a method to be developed to estimate the extent of pulmonary contusion injury caused by any particular impact.

This paper describes the proposed lung injury mechanism showing how it may be explained and modelled. Extensive use has been made of the 2-dimensional dynamic finite element code DYNA2D[2] and its 3-dimensional equivalent DYNA3D[3] as well as the system modelling package GENDYN[4].

2. LUNG INJURY SCHEME - DESCRIPTION

The sequence of events which is believed to result in contusion injury is shown on Figure 1.

2.1 INITIAL CONTACT BETWEEN THORAX AND IMPACTOR

The thorax and the impactor come into contact. The impactor may be a projectile which strikes an essentially stationary thorax or it may be a stationary object (such as a steering wheel) which is struck by a moving thorax. Alternatively, both impactor and thorax may have initial velocities.

2.2 DEFORMATION OF THE THORACIC CAVITY

The impact gives rise to deformation of the chest wall and may also involve motion of internal organs. The combined effect is a change in the internal shape of the chest cavity, this shape varying with time.

2.3 GENERATION OF PRESSURE WAVES AT THE PERIPHERY OF THE LUNG

When the periphery of the lung is given a velocity normal to the surface (such as that due to thoracic cavity deformation) then pressures are generated at the surface. Under impact conditions the pressures generated by imposed motion are invariably very much larger than any pressures due to overall change in the volume of the lungs.

2.4 PROPAGATION, REFLECTION AND INTERFERENCE OF PRESSURE WAVES

The pressures generated at the periphery of the lung propagate through the parenchyma as a wave, in much the same way as ripples spread outwards from a pebble dropped into a pond. The speed of propagation will be at or a little above the speed of sound in the lung depending on the pressure.

As the pressure waves travel through the parenchyma they may impinge on the inside of the chest cavity, meet and interfere with other pressure waves or be concentrated (and hence amplified) in particular regions of the lung. The net result will be a complex distribution of pressure varying both spatially and temporally. Thus, if pressure were to be measured at points in the lung then different histories would be found at different points and these would have different rates of pressure rise and maximum pressure.

2.5 GENERATION OF DIFFERENTIAL PRESSURES ACROSS ALVEOLAR SEPTA

The pressure measured at points along a line across the lung would, taken as a whole, appear to be a smooth curve. However, if the curve were examined more closely then it would be seen to consist of a series of plateaux with step changes between. Within each alveolus the pressure is more or less constant and the step changes in pressure occur between alveoli, across the alveolar septa. Thus there is, in general, a pressure differential across each septum with a higher pressure on one side than on the other.

2.6 BURSTING PRESSURE WITHIN CAPILLARIES

The pressure differentials across alveolar septa give rise to pressures within the capillaries which are higher than the pressure in the surrounding alveoli. If these pressures are high enough then they will lead to bursting of the capillaries.

2.7 FLOODING OF PARENCHYMA - CONTUSION INJURY

Burst capillaries allow red cells to flood into the alveoli. The cells lost from a given capillary may remain in one alveolus or may flow via the alveolar ducts into adjacent alveoli. Either way, it is the flooding of alveoli with red cells from burst capillaries which is taken to constitute contusion injury.

3. LUNG INJURY SCHEME - EXPLANATION AND MODELLING

3.1 POST-IMPACT DEFORMATION OF THE THORACIC CAVITY

Whilst it is self-evident that chest cavity deformation will take place when thoracic impact occurs, it is necessary to make a quantitative prediction of the deformation history if useful estimates of injury are to be possible.

The work on which this paper is based has been concerned with impact of small high speed projectiles on the thorax. DYNA3D has been used to model chest walls and to predict the extent of deformation after impact. However, an alternative and better method for this type of impact has been the spring-mass-damper model shown on Figure 2.

This model consists of two masses which represent the impactor (M_1) and the effective mass of the chest wall (M_2). The compressive stiffness and damping of the chest wall material itself are represented by the springs K_1 and K_2 and the damper C_1. The stiffness and damping of the chest as it bends are modelled by K_3, K_4, C_2 and C_3. The impactor is given an initial velocity and the motion histories of the outer surface of the chest wall at the impact point and the inner surface immediately behind the impact point are then given by the displacement histories X(t) and Y(t) respectively.

The system modelling package GENDYN has been used to analyse the model and typical results which show excellent agreement with experimental data are shown on Figure 3.

This gives the motion history at the impact point but clearly chest wall deformation is not confined to this area alone. The observed deformed shapes of the thoracic cavity can be represented by a sinusoidal variation of deflection as one moves away from the impact point (up to half a wavelength distance from the impact point). Under other types of thoracic impact (such as car accidents) a revised model would be required and further work would be needed to determine representative deformed shapes.

3.2 GENERATION, PROPAGATION AND REFLECTION OF PRESSURE WAVES

Figure 4 shows the outline of a typical 2-dimensional section through a porcine lung. A deformation history and deformed shape have been determined using the method presented in section 3.1 above and have been applied to a DYNA2D model of the section.

Each post-impact view of the model shows contours of pressure at equal pressure intervals and a "ripple" pressure wave can be clearly seen to spread out from the impact point, impinge on the lung-liver interface and reflect back into the parenchyma. The reflected wave then interferes with the incoming wave, further reflection and concentration occurs and the net result is a complex pressure distribution.

There are two important features of the behaviour.

3.2.1 Position of Most Severe Pressure History

The pressure waves originate at the surface of the lung and so the level of pressure generated here clearly determines the pressure developed later in the rest of the lung. However, multiple reflection and concentration means that, in general, the most severe pressure history is not found at the impacted edge but elsewhere in the parenchyma. Figures 5 and 6 show time histories of pressure and rate of change of pressure (dP/dt) at two positions in a typical lung model. The solid line shows results at a point very near to the impact point whilst the broken line shows the history at a point near the opposite (right hand) face of the model. It can be seen that the latter position suffers a higher maximum pressure and also a higher maximum value of dP/dt.

3.2.2 Pressure Generated at the Periphery of the Lung

It has been found that the pressure generated at the deformed edge of the lung (and hence the pressures developed elsewhere in the lung) is almost entirely dependent upon the velocity of deformation and bears little or no relation to the overall chest

cavity deformation or the change in lung volume. This is a significant result since it explains why impact velocity is a more important criterion than extent of chest deformation.

Figure 7 shows the relationship between applied velocity and generated pressure for a typical composition of lung and it is clear that high velocity chest deformation (due to high velocity impacts) will give rise to much higher intra-thoracic pressures than low velocity deformation.

3.3 GENERATION OF TRANS-SEPTAL PRESSURE DIFFERENTIALS

At the macroscopic level the lung may be considered to be an essentially homogeneous medium through which pressure waves would be expected to propagate in a reasonably smooth manner. Under the microscope the parenchyma can, of course, be seen to be nothing of the kind. Instead, in traversing the lung one would encounter alternate "layers" of air (alveoli) which is compressible and of negligible density and a mixture of tissues and fluids (alveolar septa, capillaries, etc) which together are relatively incompressible and massive. Generation of pressure differentials has been investigated by considering the transmission of pressure through a multilayer sandwich of air (alveoli) and tissue (alveolar septa - assumed to have properties similar to those of water).

DYNA2D has been used to model the small region of parenchyma shown on Figure 8. Typical dimensions of 45μm alveolar diameter and 5μm septal thickness have been used. The whole model is initially at atmospheric pressure (1.0 atm) and one end is instantaneously raised to 1.1 atm and held at that level.

As can be seen from the three pressure profiles, the pressure pulse does not flow smoothly through the model. With the exception of the first alveolus (which is subject to various "edge effects") the pressure within any given alveolus is essentially constant and step changes occur between alveoli. Two particular features should be noted.

3.3.1 Speed of Sound

The speed of sound in air at 1.0 atm is about 340 m/s whilst that in water is 1500 m/s. Pressure waves, which will propagate at or a little above the speed of sound, might therefore be expected to propagate along the model at a speed somewhere between 340 m/s and 1500 m/s. However this is not the case, the actual speed of propagation being about 40 m/s.

This result can be explained by considering the overall physical properties of a material which is composed of 90% air and 10% water. The air controls the overall compliance (reciprocal of stiffness) whilst the density is primarily due to the water.

Under these conditions, theory shows that the speed of sound at atmospheric pressure is given by,

$$C = \sqrt{\frac{Po\ \gamma}{x\ (1-x)\ \rho_w}}$$

where, C = speed of sound
Po = pressure = 1 atm
γ = 1.4 for air
ρ_w = water density = 1000 kgm^{-3}
x = proportion of water = 0.10

This gives C = 39.4 m/s which is in agreement with the observed behaviour.

3.3.2 Pressure Difference

In general the pressure waves being transmitted through the parenchyma are not as steep-fronted as the test pulse described above but instead have a rate of rise which is low in relation to the transit time of a pressure pulse across an alveolus. In such cases, the pressure difference across each alveolar septum is approximately given by,

$$\delta P = \frac{(W+T)}{C}\ \frac{dP}{dt}$$

where, δP = pressure differential
C = speed of pressure wave propagation
W = alveolus diameter
T = alveolar septum thickness
dP/dt = rate of change of pressure

It is important to note that under these conditions the pressure differential is a function of dP/dt and not of pressure itself. For higher rates of pressure rise (dP/dt > 25000 atm/s seems to be a reasonable cut-off) the expression will tend to estimate lower pressure differentials than the DYNA2D models although the discrepancy is usually relatively small.

3.4 BURSTING PRESSURE WITHIN CAPILLARIES

Microscopic examination of contused lungs shows accumulation of red blood cells in the alveoli but conclusive evidence of complete rupture of alveolar walls cannot be found. This suggests that blood is released by bursting of capillaries due to internal overpressure rather than by being ripped apart during failure of the alveolar septa of which the capillaries are a part.

It is clear from Section 3.3 that generation of pressure differences between component parts of the parenchyma is an integral part of the pressure transmission mechanism. Therefore, it is quite reasonable to suppose that pressure differences will be generated between capillaries and the adjacent alveoli. However, the mechanism by which these pressures are produced is not yet fully understood and so it is not yet possible to make quantitative predictions.

It is nonetheless clear that a capillary would be expected to burst when the pressure differential across the septum reaches some critical value (V_{crit} say). The value of V_{crit} will depend on capillary strength and also capillary dimensions, particularly the ratio between capillary diameter and wall thickness, larger capillaries with thinner walls having a lower value of V_{crit} than smaller ones with thicker walls.

3.5 PREDICTION OF CONTUSION DAMAGE

The ideas presented above allow a prediction to be made of whether or not a particular capillary will burst under a given impact. If values of V_{crit} in Section 3.4 were determined for a large number of capillaries then it would be reasonable to expect that the results would follow a normal distribution with some mean M and standard deviation S. The probability that at any particular point in the lung a capillary chosen at random would burst is then given by,

$$\text{Prob} (DP > X) = P \text{ (say)}$$

where, DP = maximum pressure differential
X = normally distributed random variable with mean M and standard deviation S

Suppose that a capillary failure only affects the alveolus which contains it and that I out of the N capillaries in each alveolus need to burst before sufficient blood flows into the alveolus to render it "damaged". Then the probability that an alveolus chosen at random will be "damaged" by the impact (D say) is given by,

$$D = \sum_{r=I}^{N} \frac{N!}{r!\,(N-r)!} P^r (1-P)^{N-r}$$

D is also the proportion of alveoli which would be damaged in the area being considered and so it can be seen that a "map" can be built up of percentage damage in different areas of the lung under any given impact conditions.

4. CONCLUSIONS

Mechanisms involved in the occurrence of pulmonary contusion injury due to non-penetrating thoracic impact have been presented. In most cases the mechanisms can be explained by reference to simple analytical expressions or can be demonstrated using finite element or other mathematical models. The principle area where there is still some uncertainty is the level of bursting pressure generated in capillaries as pressure waves pass through the lung.

The lung damage scheme has enabled many observed results to be explained. In particular the dependence on impact velocity, the relative unimportance of maximum deformation and the reasons why the most serious injury need not be at the impact point are now understood.

Most of the features needed to produce a tool capable of giving quantitative estimates of pulmonary contusion injury under given impact conditions are now in place. The next stage will be to compare results from specific experiments with analytical predictions to refine the scheme further. This will enable some of the "grey" area surrounding the final stages of the damage mechanism to be clarified.

5. ACKNOWLEDGEMENTS

The authors are indebted to the Chemical Defence Establishment, MOD (PE), Porton Down, England who have sponsored the study upon which this paper is based and have given permission to publish. CDE have also carried out the experimental work against which the findings of the study have been correlated and special thanks are due to R.L. Maynard and G.J. Cooper of CDE whose specialist advice and assistance have been invaluable.

6. REFERENCES

1) Cooper G.J., Maynard R.L. 'An Experimental Investigation of the Biokinetic Principles Governing Non-Penetrating Thoracic Impact to the Chest and the Influence of the Rate of Body Wall Distortion upon the Severity of Lung Injury.', Ministry of Defence, Procurement Executive, Chemical Defence Establishment, Porton Down, England.

2) Hallquist J.O. 'User's Manual for DYNA2D - An Explicit Two-Dimensional Hydrodynamic Finite Element Code With Interactive Rezoning', Lawrence Livermore Laboratory, University of California, January 1984.

3) Hallquist J.O., Benson D.J. 'DYNA3D User's Manual (Non-Linear Dynamic Analysis of Structures in Three Dimensions)', Lawrence Livermore Laboratory, University of California, March 1986.

4) 'GENDYN User Guide', Frazer-Nash Consultancy Limited, Leatherhead, England, May 1987.

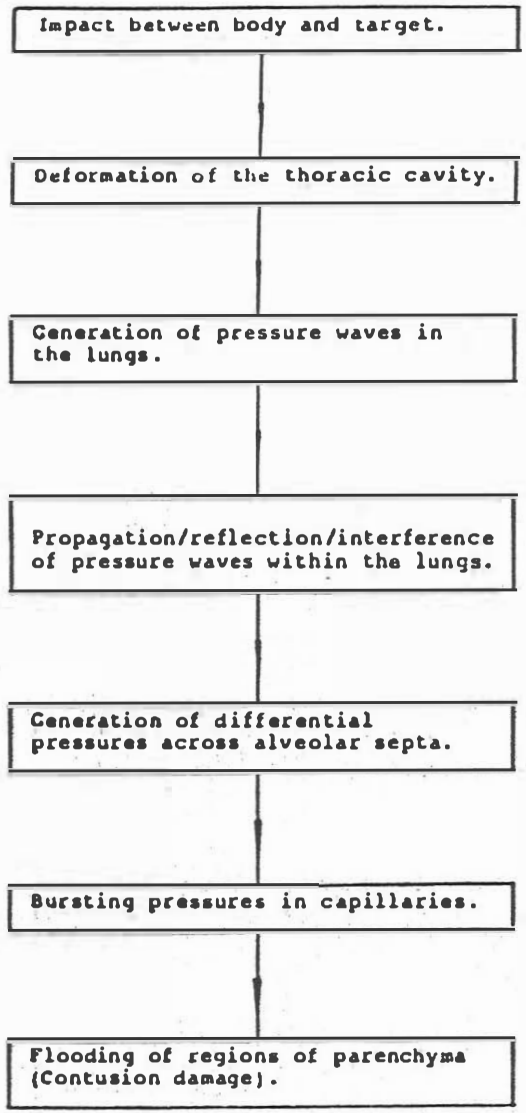

Figure 1: LUNG DAMAGE SCHEMATIC

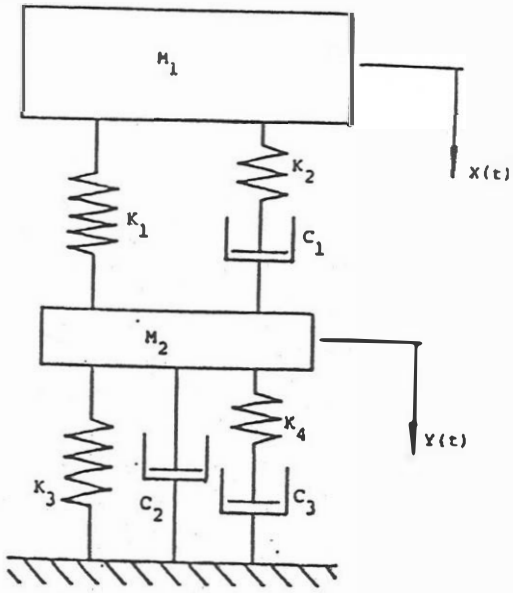

Figure 2: GENDYN CHEST DEFORMATION MODEL

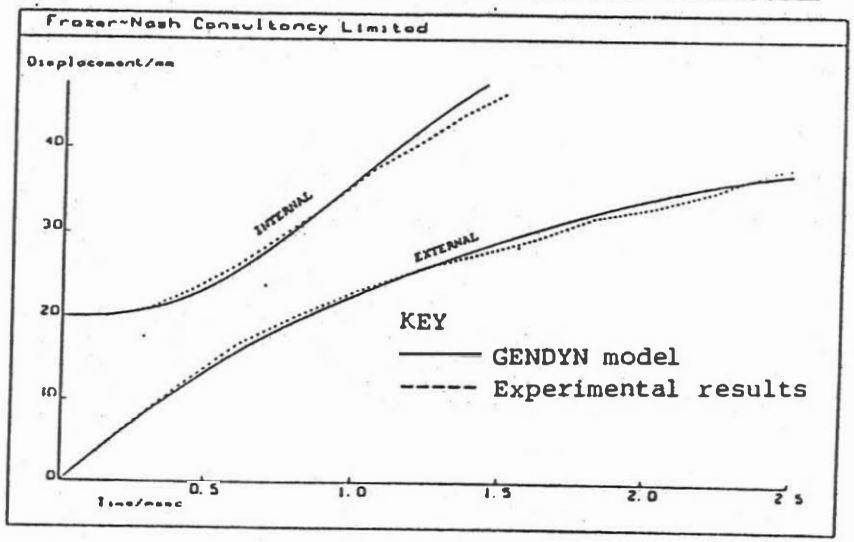

Figure 3: RESULTS FROM GENDYN CHEST DEFORMATION MODEL

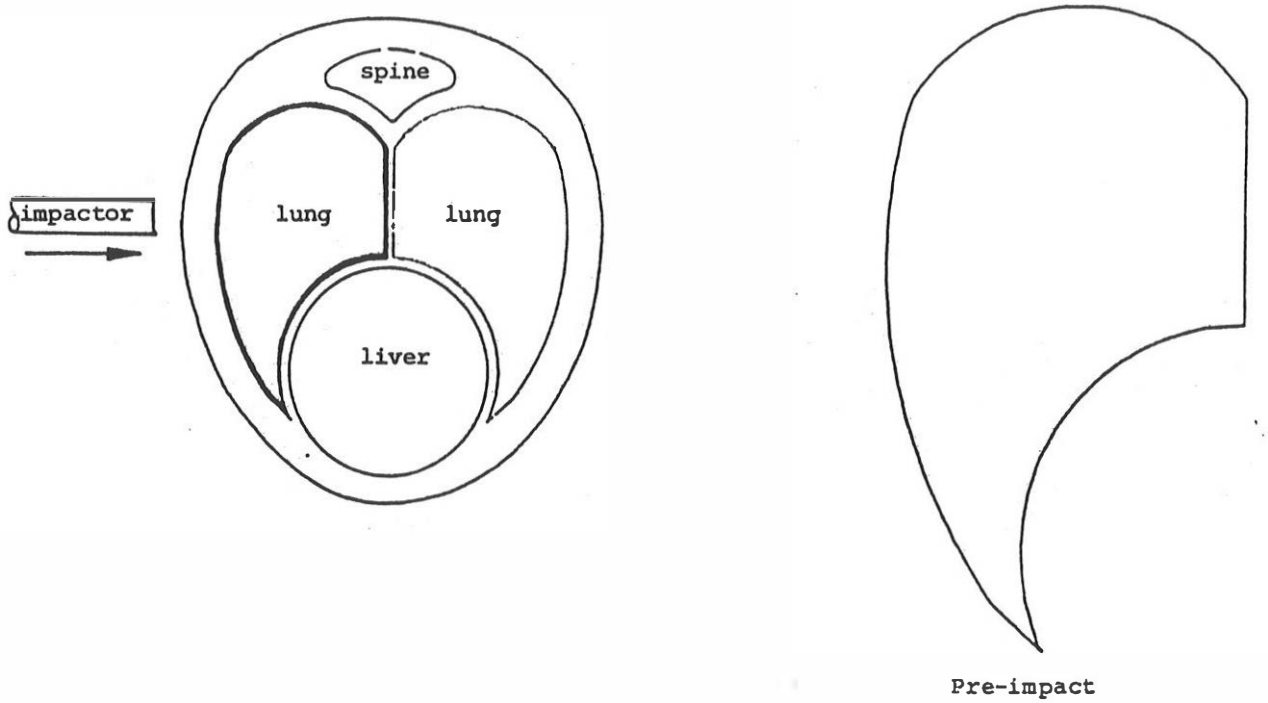

Figure 4 : DYNA2D LUNG SECTION RESULTS

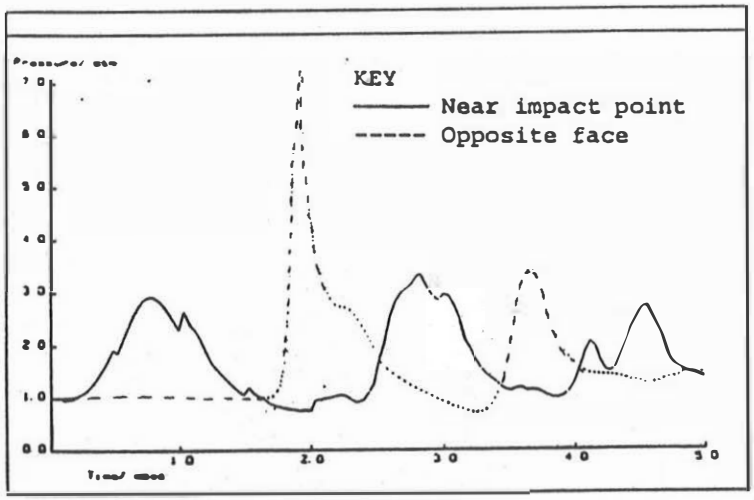

Figure 5 : DYNA2D PRESSURE HISTORIES

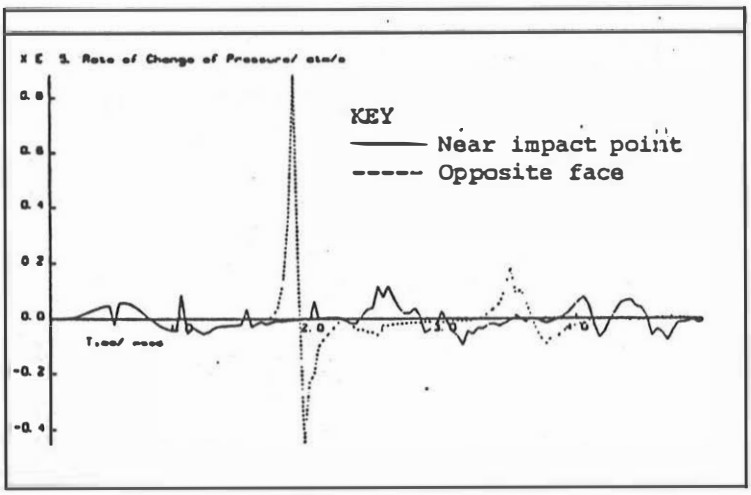

Figure 6 : DYNA2D dP/dt HISTORIES

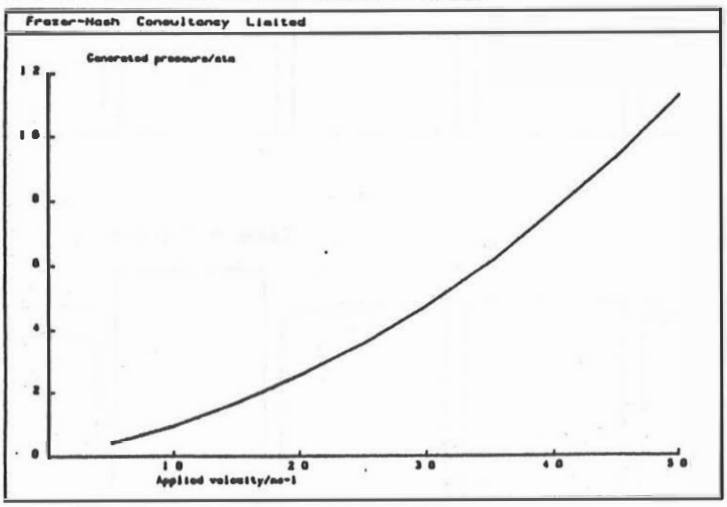

Figure 7 : RELATIONSHIP BETWEEN VELOCITY AND GENERATED PRESSURE FOR TYPICAL LUNG

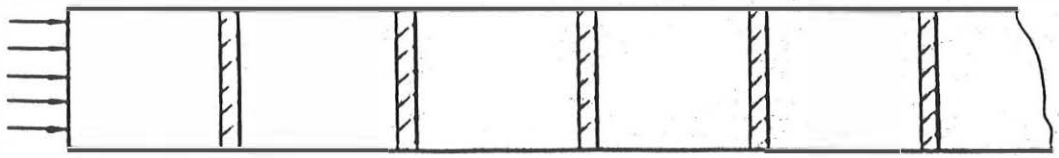

Air (alveoli)

"Water" (alveolar septa)

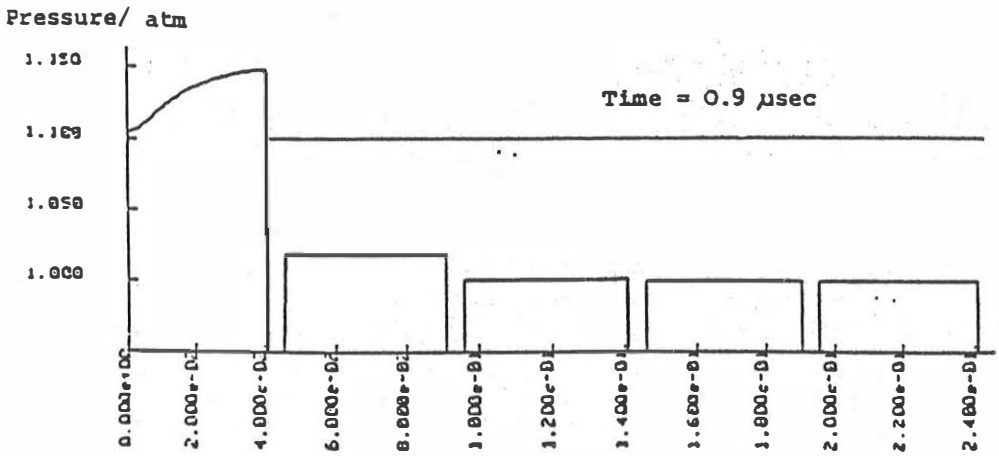

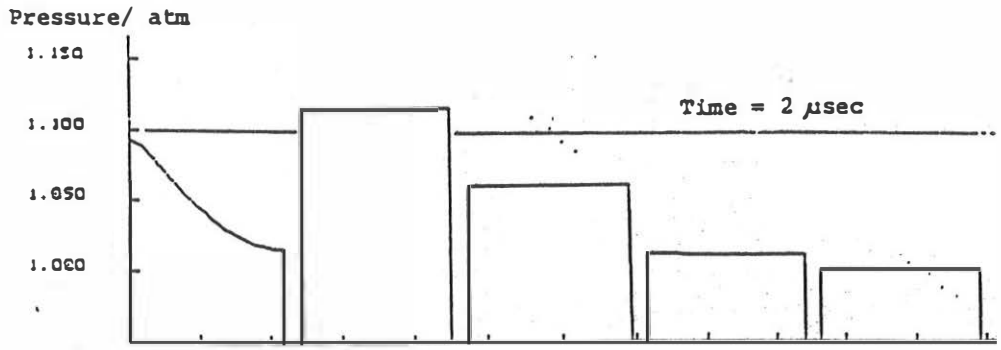

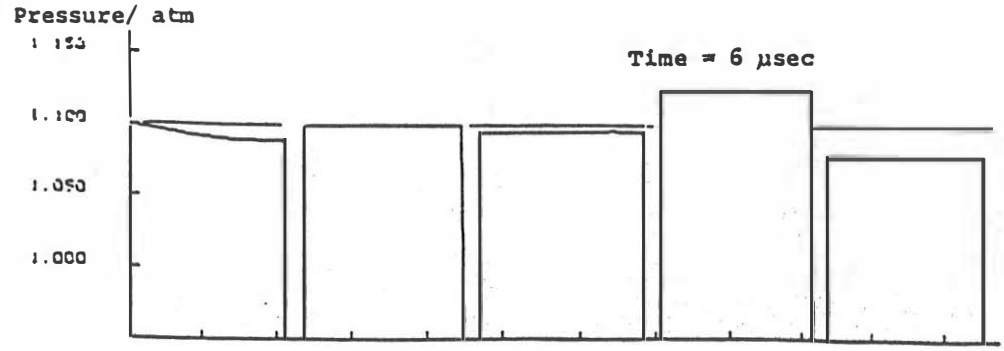

Figure 8 : GENERATION OF PRESSURE DIFFERENTIALS ACROSS ALVEOLAR SEPTA